DOI: 10.21062/mft.2025.063 http://www.journalmt.com

Temperature Matters: Annealing Effects on Silver Protection and Tungsten Oxidation in W@Ag Core-Shell Powder

Angelina Strakošová (0000-0002-1276-7263)[1,2], Pavel Lejček (0000-0002-6870-0949)[1], Ilona Voňavková (0000-0001-6196-7811)[2], Vojtěch Dalibor (0000-0002-6910-3206)[2]
[1]Institute of Physics, Czech Academy of Sciences, Na Slovance 2, 182 00 Praha 8. Czech Republic. E-mail: strakosova@fzu.cz, lejcekp@fzu.cz
[2]Department of Metals and Corrosion Engineering, University of Chemistry and Technology, Technická 5, 166 28 Praha 6. Czech Republic. E-mail: strakosn@vscht.cz, vonavkoi@vscht.cz, vojtechd@vscht.cz

Core-shell powders have been extensively studied due to their complex structure and wide range of applications. W@Ag core-shell powders are particularly interesting due to the synergy between the tungsten and silver, which can be beneficial in the electronics industry. However, knowledge of their thermal stability is limited, particularly concerning the impact of annealing temperatures on structural integrity and oxidation resistance. In this work, W@Ag core-shell powder was heat-treated in the temperature range 100–700 °C for 1 h in air. Investigation of the microstructural changes using scanning electron microscopy equipped with energy-dispersive X-ray spectroscopy showed that the limiting temperature is 500 °C, when the shell began to decompose and the core began to oxidize. Moreover, X-ray diffraction analysis determined that the phase composition of the thus heat-treated material consisted of approximately 50 % Ag and 50 % Ag_2WO_4.

Keywords: Tungsten, Silver, Core-shell powder, Annealing, Oxidation

1 Introduction

Core-shell particles are a group of materials that are characterized by a bimodal structure. In general, the core and the shell are usually two different materials [1]; however, these two parts could also be a combination of the same material with nano and microstructure [2]. Moreover, the shell is always a solid state organic or inorganic material, whereas the core could be in a solid as well as liquid or gas state [3]. Thanks to the possibility of combining two completely different materials, core-shell powders are widely used in pharmaceutical and biomedical applications, cosmetic and food industry, environmental monitoring, and material science [3-5].

Recently, a huge interest has been focused on the investigation of nanoparticles with a core-shell structure [5-9]. However, there is a lack of work dedicated to core-shell microparticles. Moreover, there is a limited number of papers describing the structure and properties of the core-shell powder that combines diametrically different materials: a W core and Ag shell. The combination of these materials is very interesting in terms of use in electronics, e.g, as electrical switches [10], where W serves as a hard material with high resistance to erosion and welding, while Ag serves as a ductile component with excellent thermal and electrical conductivity [11]. Nevertheless, the combination of W and Ag was described in Ref. [12], where the authors attempted to produce an Ag/W composite from powder, while the Ag/W nanowire composite networks are studied in Ref. [13]. Some works [14, 15] describe the production and characterization of Ag@WO_3 nanopowder. W–Ag and W–Cu–Ag nanopowders with a core-shell structure and composites produced from these powders are characterized in the work [16]. A highly dense W–Ag composite was prepared from Cu@Ag@W powders with a size of a few micrometers by the authors of [10]. W@Ag core shell powder with grain sizes in the range of tens of micrometers has so far been described in work [17]. The heat treatment of Cu@Ag core-shell powders was described in Refs. [18, 19]. A few micrometer-sized Cu@Ag core-shell powders were studied in work [18]. The authors found that temperatures below 160 °C have minimal effect on the Ag shell; temperatures in the range of 160–250 °C cause the formation of Ag necks between particles; and temperatures above 250 °C lead to the dewetting of the powder's shell, which causes the formation of Ag particle clusters and free oxygen access to the core material. Dewetting and agglomeration effect of Ag shell was also described in the case of nanometer-sized Cu@Ag powders, already at a temperature of 200 °C [19].

Since the silver should act as a protective layer on tungsten, it is therefore intriguing to know what temperature is limiting when no destruction of the W@Ag core-shell structure and oxidation of the W core is observed. This research provides a qualitative overview of the microstructural changes occurring in

the W@Ag core-shell powder during annealing in the temperature range of 100–700 °C in air.

2 Experimental

Commercially produced W@Ag core-shell powder was used in this work. The main characteristics of the powder are described in detail in Ref. [17]. The powder was annealed at temperatures ranging from 100 to 700 °C for 1 h in air, followed by slow air cooling in the furnace. For this purpose, the laboratory electric resistance furnace (MARTINEK MP05, Czech Republic) was used. The maximal temperature of 700 °C was chosen because it was the temperature of the metal matrix composite production [17].

Annealed powder was studied in terms of morphological and microstructural changes using a scanning electron microscope (SEM, Tescan Mira, Czech Republic) equipped with energy-dispersive spectroscopy (EDS, Oxford Instruments X-Max 20, United Kingdom). To observe the morphology, the annealed W@Ag powder was attached to the carbon tape. For the microstructural observation, the powders were cold-embedded into Technovit 5071 resin; then the samples were ground on SiC papers (PP 400–2500) and polished using diamond suspension with 3 and 0.25 μm particle sizes. To better electron conductivity during SEM observation, all samples were coated with 5 nm of Au using a Quorum Q150R ES (Quorum Technologies, UK) machine. The fact of the Au coating was taken into account when evaluating the chemical composition of core-shell powders by EDS. X-ray diffraction analysis (XRD) was performed to determine the phase composition of W@Ag powders after heat treatment at 500–700 °C using a PANalytical X'Pert PRO instrument (Co anode; generator settings - 30 mA, 40 kV; step size 0.0390; 2θ angle range 6–109°).

Moreover, samples of W–Ag metal matrix composite (MMC) were heat-treated at 500 and 700 °C for 1 h in air to investigate the effect of critical temperatures (see Results and Discussion section) on the changes in the MMC structure. The samples were shaped as cuboids, measuring 4 x 4 mm in cross-section and 6 mm in height. Heat-treated samples were cut at mid-height, ground and polished; and then their microstructure was observed using SEM.

3 Results and Discussion

The recent study [17] shows that the W@Ag core-shell powder is characterized by a spherical shape with an orange-like, in some cases defective, surface. The mean size of the powder was measured to be 37.1 μm. The microstructure of the W@Ag consisted of a pure W core with a pure Ag shell according to the SEM/EDS results. Moreover, the adhesion between the core and the shell is quite poor, which comes through the presence of holes in the W/Ag interface [17].

Figure 1 shows the microstructure of the W@Ag core-shell powder after being heat-treated at temperatures of 100–300 °C for 1 h. It can be seen that the temperatures have no effect on the changes of the powder microstructure; powders keep their shape and integrity, also bad adhesion between the core and shell is visible in Fig. 1 (red arrows), which was also described in Ref. [17]. The temperature of 200 and 300 °C caused random partial sintering of individual particles (Fig. 1b). Nevertheless, the integrity of the Ag shell was preserved. This means that Ag is stable and also has a protective effect against the W core oxidation at 100–300 °C.

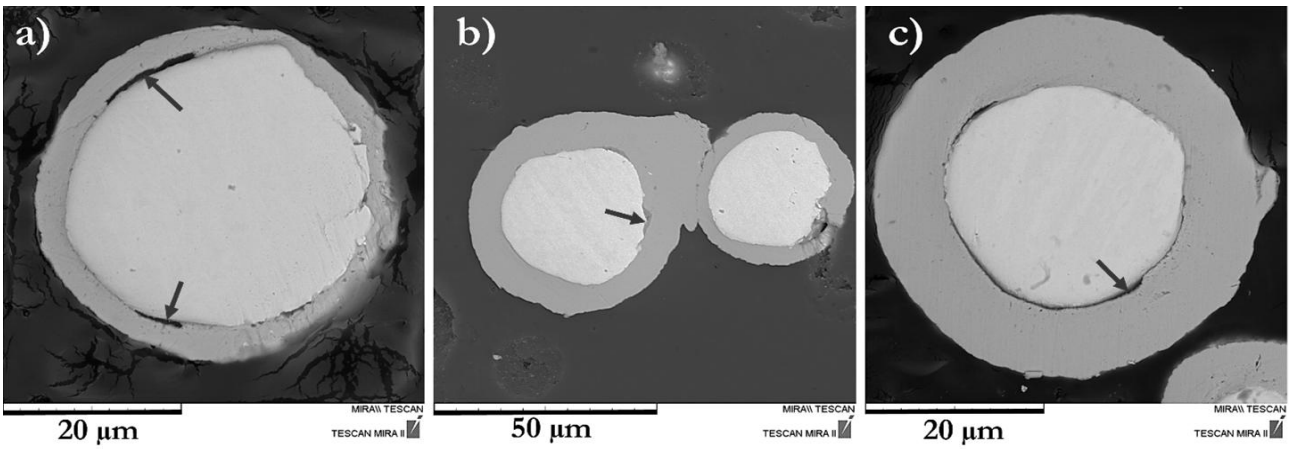

Fig. 1 *Microstructure (SEM images) of the W@Ag core-shell powder particles after being heat-treated at: a) 100 °C, b) 200 °C, c) 300 °C*

Besides the protective effect of the Ag shell, Fig. 1 also shows different thicknesses of the Ag shell on the W core. Different thicknesses of the Ag shell may be explained by the way of cutting the particles, as it is shown in Fig. 2. When we have a spherical powder particle and cut it at position A, we will see a small part

of the core material and a wide zone of the shell material. The example of the A cut can be seen in Fig. 1c. The section B (Fig. 2) could be represented through the left particle shown in Fig. 1b. Finally, when the powder particle is cut in its middle part, the microstructure will consist of a thin shell layer (Fig. 2 section C and Fig. 1a). Considering this, it is complicated to measure the thickness of the shell of core-shell materials.

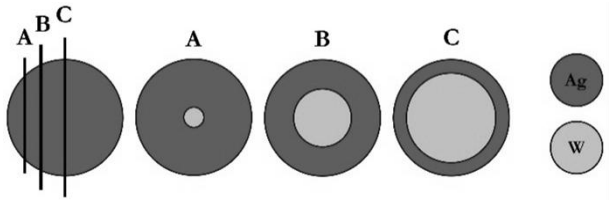

Fig. 2 *Graphical representation of powder cross-section*

Figure 3 represents the microstructure of the W@Ag core-shell powder after the heat treatment at 400 °C for 1 h. It can be seen that the situation is more complex here compared to Fig. 1. Firstly, 400 °C for 1 h in air was enough to initiate the sintering of the W@Ag powder (Fig. 3, green square) by the creation of necks between individual particles. Because the pressure was not used in our study, the obtained "bulk" material is characterized by a very defective microstructure (the presence of pores and voids) with poor mechanical properties (the material could be fractured with the hands). Because the powder was sintered, it was hard to evaluate the oxidation, since the oxygen supply to that area was limited. The situation is a bit different in the surface area, which was in direct contact with oxygen (Fig. 3, blue square). Here, the neck formation is also visible. However, the most interesting thing that can be observed is the pore formation in the Ag shell. This effect can be connected with the "dewetting and agglomeration" of the Ag described in Refs. [18, 19], which took place at lower temperatures. The temperatures of "dewetting and agglomeration" increase with the increase of powder particle size.

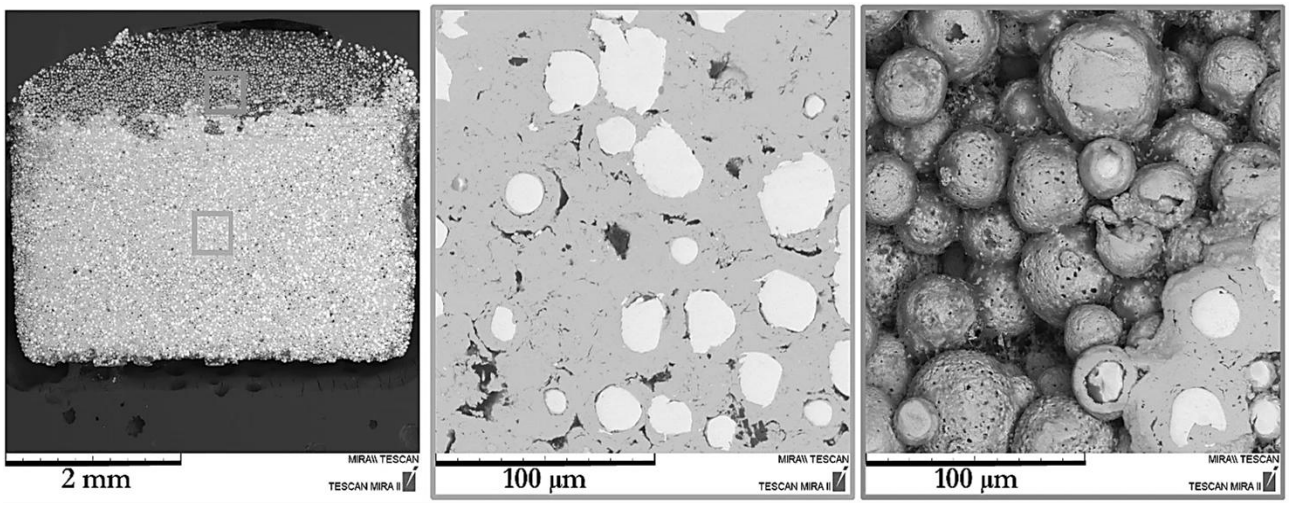

Fig. 3 *SEM micrographs of the microstructure of the W@Ag core-shell powder after being heat-treated at 400 °C*

The microstructure of the core-shell powders after the heat treatment at 500 and 600 °C for 1 h in air is depicted on SEM micrographs in Fig. 4. It can be seen that these temperatures caused noticeable changes in the particle's microstructure compared to the lower temperatures (Figs. 1, 3). According to Ref. [20], the oxidation of W takes place in the temperature range of 300–1000 °C, depending on the partial pressure of oxygen and the duration. Figure 4b shows that the temperature of 600 °C had a huge impact on the powder's microstructure, rapidly decreasing the number of the initial W cores that have not reacted with oxygen.

Figure 5 shows the detailed SEM micrographs of the W@Ag powder microstructure after being exposed to 500 and 600 °C for 1 h. Also, the EDS point analysis was performed (Fig. 5, spectra 25–47) to determine the chemical composition of heat-treated powders compared to the as-produced, which consists of a pure W core and Ag shell [17]. The results of the EDS analysis are summarized in Table 1. It is visible (Fig. 5a, Tab. 1) that the temperature of 500 °C began to initiate the oxidation of the core-shell powder. At first sight, it may seem that the W core remained untouched, and the main changes have occurred in the shell region. However, EDS analysis showed that 500 °C was high enough to rapid diffusion through the Ag shell, which agglomerated in unevenly distributed islands of pure silver (Fig. 5a, spectra 25–32) around an oxide formed by the reaction of W and O (Fig. 5a, spectra 33, 34).

SEM/EDS analysis of the W@Ag powder microstructure and chemical composition (Fig. 5b, Tab. 1) shows that the heat treatment of the powder at 600 °C caused the formation of a very thick layer of oxides around the W core of the powder.

It is visible (Fig. 6) that the temperature of 700 °C caused enormous changes in the microstructure of W@Ag core-shell powder; the uniform spherical shape of the powder particles has changed to a coarser agglomerate with an irregular shape. It can also be seen (Fig. 6) that micrometer-sized crystallites have been formed after the heat treatment of W@Ag powder at 700 °C for 1 h. The results of EDS analysis show (Tab. 2, spectra 49–52) that the crystals consist of approximately 80 wt.% of W and 20 wt.% of O, which is equal to 26 at.% of W and 74 at.% of O. This atomic concentration is very close to the concentration matching WO_3 [21]. According to the literature, spectra 33–34, 39–47 (Tab. 1) and 43–48 (Tab. 2) may show the presence of Ag/WO_3 [14, 15] or even Ag_2O/WO_3 [12] "composite". Moreover, authors of Ref. [12] found the presence of Ag_2WO_4.

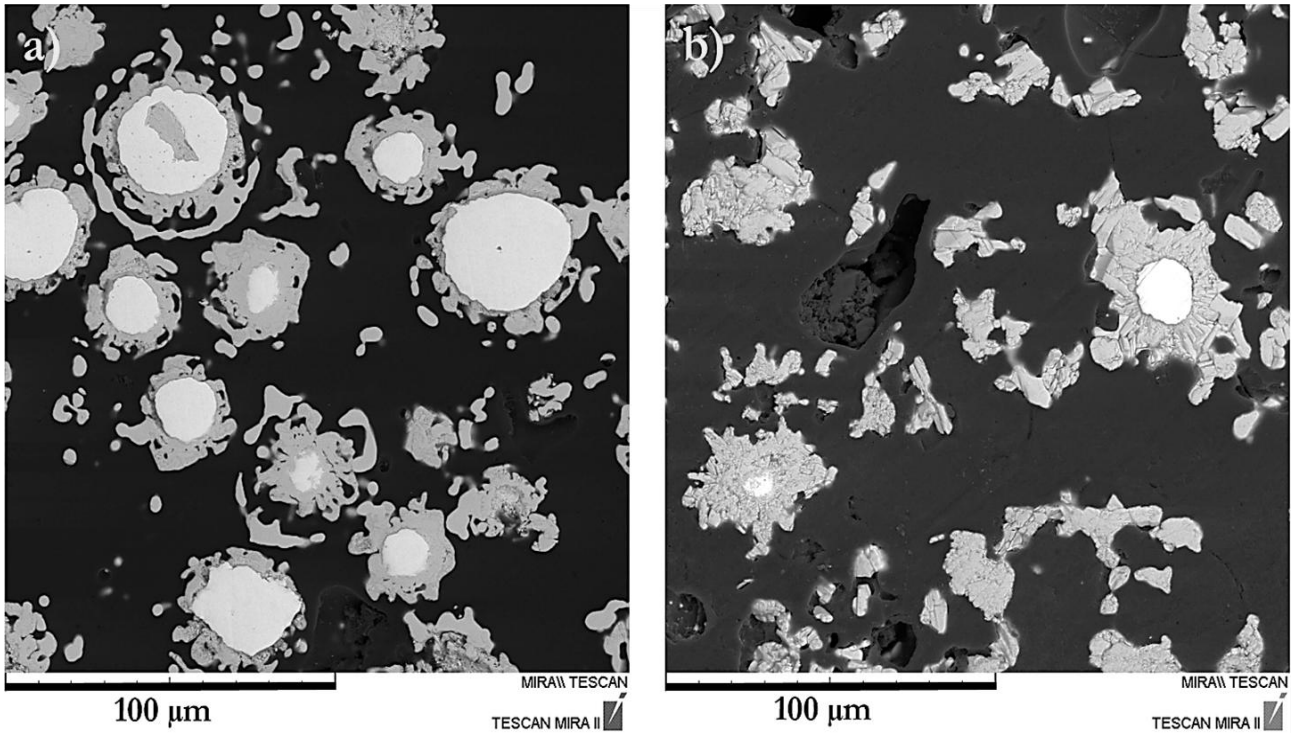

Fig. 4 *Microstructure (SEM images) of the W@Ag core-shell powder after being heat-treated at: a) 500 °C, b) 600 °C*

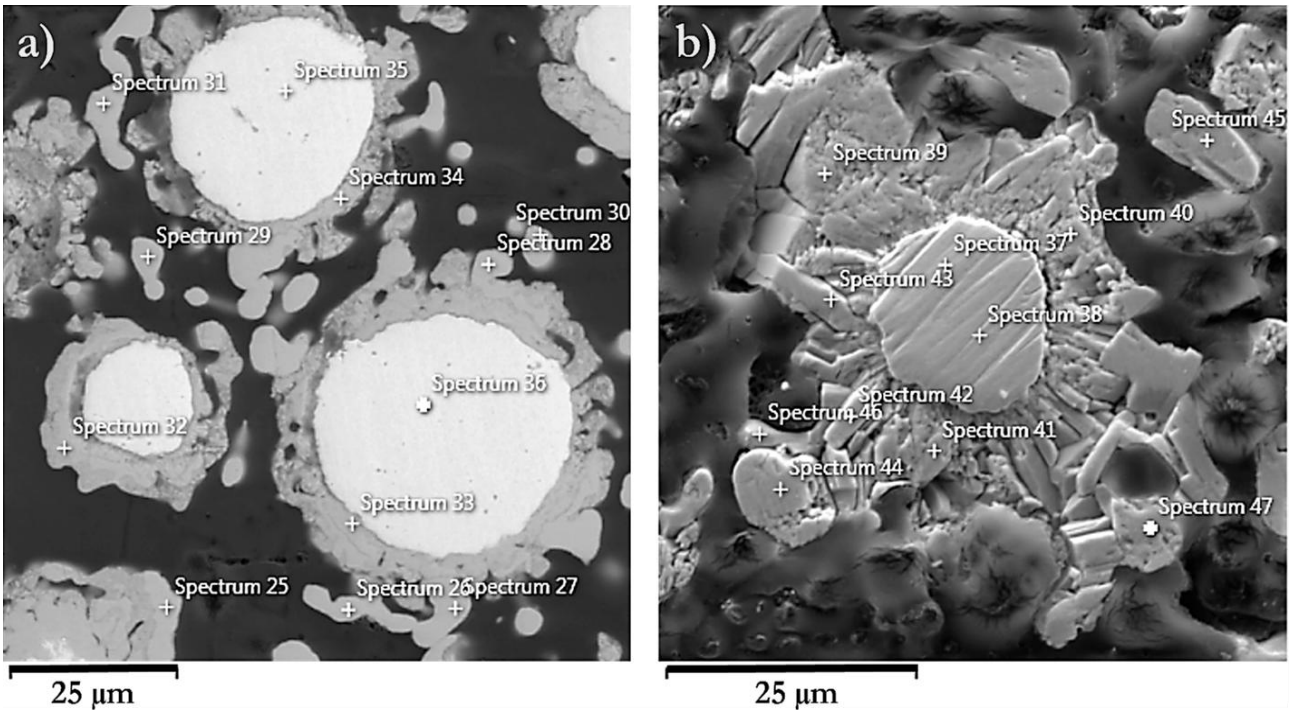

Fig. 5 *SEM images of the microstructure of the W@Ag core-shell powder after being heat-treated at: a) 500 °C, b) 600 °C*

Tab. 1 *Chemical composition of the W@Ag core-shell powder after being heat-treated at 500 °C and 600 °C (according to EDS analysis)*

	Spectrum	wt. %		
		W	Ag	O
500 °C	**25–32**	-	100.0	-
	33	57.2	29.0	13.9
	34	55.1	31.1	13.8
	35	98.9	-	1.1
	36	100.0	-	-
600 °C	**37–38**	100.0	-	-
	39	60.9	21.8	17.4
	40	56.3	28.7	15.0
	41	55.5	28.9	15.6
	42	59.4	22.0	18.6
	43	62.6	21.0	16.4
	44	61.3	22.8	16.0
	45	62.3	20.4	17.3
	46	63.3	25.4	11.3
	47	58.1	27.8	14.1

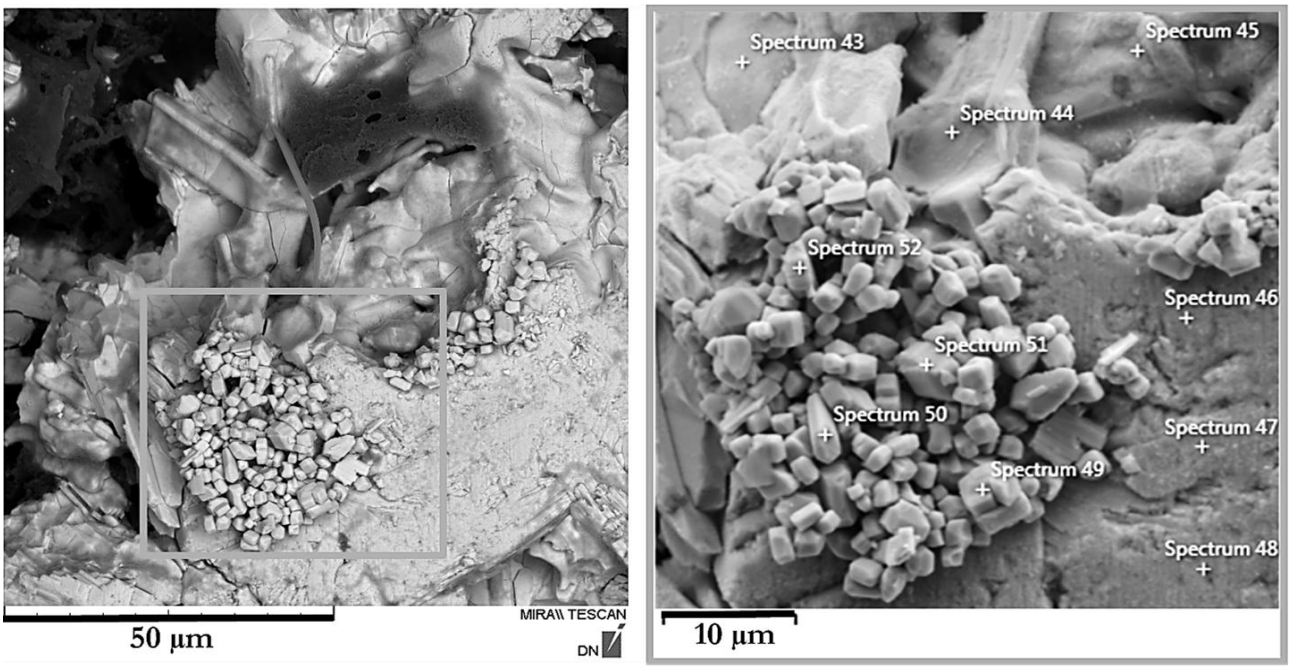

Fig. 6 *SEM micrographs of the microstructure of the W@Ag core-shell powder after being heat-treated at 700 °C*

Tab. 2 *Chemical composition of the W@Ag core-shell powder after being heat-treated at 700 °C (according to EDS analysis)*

Spectrum	wt. %		
	W	Ag	O
43	52.9	22.2	24.9
44	45.8	32.0	22.1
45	38.8	40.2	21.0
46	59.9	22.0	18.0
47	59.0	24.0	17.0
48	53.4	31.2	15.4
49	77.3	-	22.7
50	86.4	-	13.6
51	76.4	-	23.6
52	78.1	-	21.9

XRD patterns of the W@Ag core-shell powder heat-treated at 500–700 °C are shown in Figure 7. It is evident that the powder heat-treated at 500 °C is characterized by the presence of three phases, the semiquantitative percentage of which was determined as follows: 48 % of Ag, 1 % of W and 51 % of Ag_2WO_4. It is also visible that temperatures of 600 and 700 °C caused a decrease in the Ag peaks, but an increase in the Ag_2WO_4 peaks. Moreover, many more or less intensive peaks appear in the XRD patterns in both cases. Peaks, in the case of the temperature of 600 °C in the range of 2θ: 20–35° and 40–75°, refer to the presence of Ag_2WO_4, $Ag_2W_2O_7$, $Ag_2W_4O_{13}$ phases. In contrast, peaks in the range of 2θ: 25 – 30°, 52 – 62° and 97 – 102° show the presence of the following phases: Ag_2WO_4, $Ag_2W_4O_{13}$ and WO_3. However, it was extremely difficult to determine the semiquantitative phase composition for powders heat-treated at 600 and 700 °C as many peaks overlapped each other.

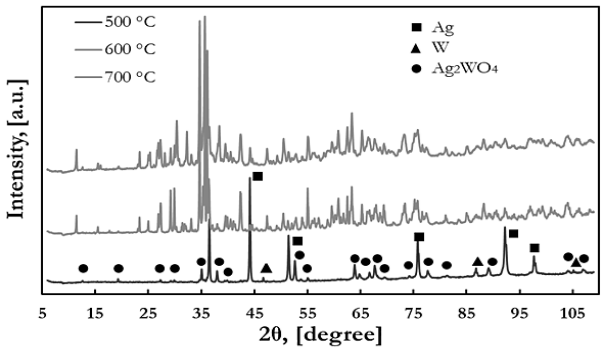

Fig. 7 *Representative XRD patterns showing the phase composition changes of the W@Ag*

As mentioned above, the Ag shell serves as a protective layer against oxidation. The process of oxidation of the W core in W@Ag core-shell particles is thus primarily driven by the diffusion of O through the Ag shell and the subsequent reaction with the W core. Both these steps are temperature-dependent. In addition, the effectiveness of the protection ability of the Ag layer also decreases with temperature. For example, it agglomerates into drops at the Cu surface, thus opening the core to direct contact with O2 [19]. In the case of W@Ag particles, we did not observe such agglomeration, but formation of extensive pores appeared after annealing at 400 °C (Fig. 3c).

We can estimate the amount of O diffusing through the Ag layer during 1 h annealing at individual temperatures. For the diffusivity, we can refer to papers [22-24]. The diffusion could be affected by the defectiveness and grain size of the Ag shell. More defective and finer-grained microstructure will promote better diffusion rate, not only of oxygen in the case of this work through the material layer, but also the self-diffusion [25].

Accepting the expression for the temperature dependence of diffusion of O in Ag.

$$D_{O\rightarrow Ag}(T) = D_{0,O\rightarrow Ag}\exp\left(-\frac{Q_{O\rightarrow Ag}}{RT}\right) \quad (1)$$

The parameters O diffusion in Ag are $D_{0,O\rightarrow Ag}$ = 4.9 × 10^5 μm² s^{-1} and $Q_{O\rightarrow Ag}$ = 48.5 kJ mol^{-1} [26]. The values of the O diffusivity, $D_{O\rightarrow Ag}(T)$, are listed in Table 3 for individual temperatures of interest. Supposing the W/Ag volume ratio being 1:1, the diameter of the core is 29.4 μm and the thickness of the Ag shell is 3.9 μm. As the partial pressure of O in the atmosphere is 0.2 bar, the number of moles in a volume also changes with temperature (cf. Tab. 3). Then the diffusive flux, *J*, of O is:

$$J(T) = D_{O\rightarrow Ag}(T)\nabla c_O(T) \quad (2)$$

Where $\nabla c_O(T)$ is the gradient of O concentration. Its rough maximum estimate is listed in Tab. 3. In these calculations, it is assumed that O does not accumulate at the Ag/W interface. This is acceptable as O can quickly diffuse and dissolve in W [27]. Finally, we can estimate the maximum O surface concentration at the Ag/W interface after annealing for the period τ = 3600 s.

$$c_{I,O}(T) = J(T)\frac{S_I\tau}{S_I} = J(T)\tau \quad (3)$$

The values of $c_{I,O}(T)$ are also listed in Tab. 3.

Tab. 3 *Diffusivity of O in Ag at temperatures 100 °C to 700 °C and estimated concentration at the Ag/W interface*

T (°C)	$D_{O\rightarrow Ag}(T)$ (μm² s^{-1})	$10^{18} \times c_O(T)$ (mol μm^{-3})	$10^{12} \times J(T)$ (mol μm^{-2} s^{-1})	$10^{7} \times c_{I,O}(T)$ (mol μm^{-2})
100	0.079	6.45	0.132	0.00474
200	2.16	5.09	2.856	0.103
300	18.58	4.20	20.27	0.73
400	84.31	3.57	78.16	2.82
500	258.74	3.11	209.1	7.52
600	614.15	2.76	440.3	15.8
700	1220.44	2.47	783.5	28.2

Figure 8 shows the concentration of oxygen in silver as a function of temperature. These results can be compared with experimental data (Figs. 1 and 3–6). The temperature of 100 °C for 1h has had almost no effect on the changes of the W@Ag powder microstructure, which corresponds to the amount of

diffused O at the level of 10^{-10} mol μm^{-2}. The first insignificant changes in the microstructure were observed after heat treatment of powder at 200 and 300 °C for 1h, which corresponds to an increasing amount of diffused O by two orders of magnitude 10^{-8}–10^{-7} mol μm^{-2}. The heat treatment of the powder at 500–700 °C for 1h has resulted in the powder oxidation that corresponds to the amount of diffused O increasing from 10^{-6} to 10^{-5} mol μm^{-2}. The amount of O at the interface at the level of 10^{-7} mol μm^{-2} seems to be a critical level for the start of the oxidation of the W core at the temperature of 400 °C. The temperature 400 °C is in good agreement with the literature data dealing with the oxidation of W ([28] and reference there). Let us emphasize that the data presented in Table 3 and Figure 8 correspond to the ideal situation where all particles are characterized by the same size, morphology and ideal core-shell adhesiveness. The presented results are therefore rather qualitative, nevertheless, enabling a rational explanation of the process.

Figure 9 shows SEM macroimages of the W–Ag MMC cross-section microstructure after being heat-treated. It can be seen (Figure 9a) that the temperature of 500 °C for 1 h has almost no effect on the W–Ag structure. The sample with an initial cuboid shape remained almost unchanged, but its corners began to deform. In contrast, Figure 9b shows that the temperature of 700 °C is critical not only for the core-shell powder, but also for the MMC produced from the powder, which is manifested by the loss of its integrity as well as microstructure and phase composition.

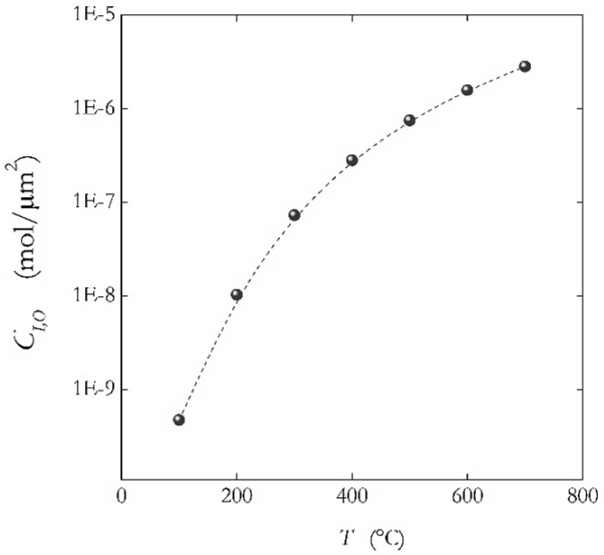

Fig. 8 *Concentration of oxygen in silver as a function of temperature*

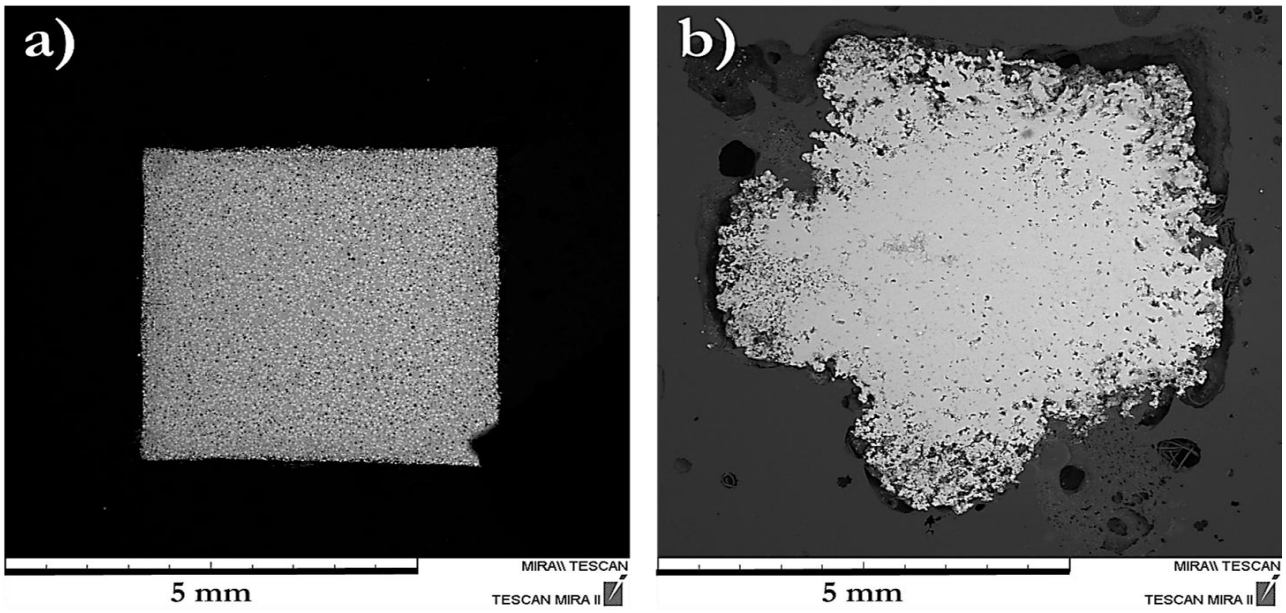

Fig. 9 *SEM macroimages of W–Ag MMC cross-section after being heat-treated at: a) 500 °C, b) 700 °C*

4 Conclusion

In this work, the thermal stability of W@Ag core-shell powder was investigated in terms of annealing temperature, focusing on maintaining structural integrity and minimizing oxidation of the W core. The conclusion of this work can be summarized as follows:

- W@Ag core-shell powders were successfully heat-treated across a temperature range of 100–300 °C for 1 hour in ambient air with no oxidation features.
- The temperature of 400 °C caused partial sintering of the W@Ag core-shell powders.
- Heat treatment of W@Ag powders at 500 °C was shown as a critical temperature where structural degradation of the core-shell structure began.

- Changes of Ag_2WO_4 oxide type to a mix of oxides $Ag_xW_yO_z$ and appearance of a new WO_3 type were observed after core-shell powder was heat-treated at 600 °C.
- The temperature of 700 °C was critical, when the core-shell powder transformed to a combination of mixed oxides.

Data availability

The data used in this manuscript are available in the Zenodo repository at the following link: https://doi.org/10.5281/zenodo.16902558.

Acknowledgement

This work was financially supported by the Czech Science Foundation under the grant No. 23-05139S. One of the authors (AS) acknowledges the grant of the Czech Academy of Sciences under No. L100102403. DV acknowledges financial support from the project "Mechanical Engineering of Biological and Bio-inspired Systems," funded as project No. CZ.02.01.01/00/22_008/0004634 by ProgrammeJohannes Amos Commenius, call Excellent Research. It was also supported from the grant of Specific university research–grant No A1_FCHT_2025_011.

References

[1] NOMOEV, A.V., BARDAKHANOV, S.P., SCHREIBER, M., BAZAROVA, D.G., ROMANOV, N.A., BALDANOV, B.R., SYZRANTSEV, V.V. (2015). Structure and mechanism of the formation of core–shell nanoparticles obtained through a one-step gas-phase synthesis by electron beam evaporation, *Beilstein Journal of Nanotechnology*, 6 (2015) 874-880.

[2] HAYES, R., AHMED, A., EDGE, T., ZHANG, H. Core–shell particles: Preparation, fundamentals and applications in high performance liquid chromatography, *Journal of Chromatography A*, 1357 (2014) 36-52.

[3] GALOGAHI, F.M., ZHU, Y., AN, H., NGUYEN, N.-T. Core-shell microparticles: Generation approaches and applications, *Journal of Science: Advanced Materials and Devices*, 5 (2020) 417-435.

[4] ZHANG, X., QU, Q., ZHOU, A., WANG, Y., ZHANG, J., XIONG, R., LENDERS, V., MANSHIAN, B.B., HUA, D., SOENEN, S.J., HUANG, C. Core-shell microparticles: From rational engineering to diverse applications, *Advances in Colloid and Interface Science*, 299 (2022) 102568.

[5] NUNZIATA, G., BORRONI, A., ROSSI, F. Advanced microfluidic strategies for core-shell nanoparticles: the next-generation of polymeric and lipid-based drug nanocarriers, *Chemical Engineering Journal Advances*, 22 (2025) 100759.

[6] GHOSH CHAUDHURI, R., PARIA, S. Core/Shell Nanoparticles: Classes, Properties, Synthesis Mechanisms, Characterization, and Applications, *Chemical Reviews*, 112 (2012) 2373-2433.

[7] KAMYSHNY, A., MAGDASSI, S. Conductive Nanomaterials for Printed Electronics, *Small*, 10 (2014) 3515-3535.

[8] KHAN, B., ELHOUSSEINI, M., AHMED, S.B., AHMAD, R.U.S., LYU, L., CHEN, H., KHAN, B., GUNASEKARAN, I., CHUHAN, F., LIU, S., YANG, Z., KHOO, B.L. Enhanced core-shell nano-conductive piezoelectric sensor via self-oriented beta phase nanocrystals for real-time monitoring of physiological signals, *Chemical Engineering Journal*, 513 (2025) 162384.

[9] GROUCHKO, M., KAMYSHNY, A., MAGDASSI, S. Formation of air-stable copper–silver core–shell nanoparticles for inkjet printing, *Journal of Materials Chemistry*, 19 (2009) 3057-3062.

[10] LUO, G., GUO, J., HU, J., LI, P., SUN, Y., SHEN, Q. Microstructure and properties of W-Ag matrix composites by designed dual-metal-layer coated powders, *Materials & Design*, 219 (2022) 110733.

[11] KESIM, M.T., YU, H., SUN, Y., AINDOW, M., ALPAY, S.P. Corrosion, oxidation, erosion and performance of Ag/W-based circuit breaker contacts: A review, *Corrosion Science*, 135 (2018) 12-34.

[12] YU, H., SUN, Y., KESIM, M.T., HARMON, J., POTTER, J., ALPAY, S.P., AINDOW, M. Surface Degradation of Ag/W Circuit Breaker Contacts During Standardized UL Testing, *Journal of Materials Engineering and Performance*, 24 (2015) 3251-3262.

[13] GAO, J.J., LIN, J.H., ZHANG, X.H., ZHU, L.P., QIN, H.L., YAO, L.G. Fabrication of assembled and welded Ag/W nanowire composite networks as electrodes for body motion monitoring and flexible heaters, *Rare Metals*, 44 (2024) 1147–1159.

[14] XU, L., YIN, M.-L., LIU, S. Superior sensor performance from Ag@WO_3 core–shell nanostructure, *Journal of Alloys and Compounds*, 623 (2015) 127-131.

[15] MA, J., MA, Z., LIU, B., WANG, S., MA, R., WANG, C. Composition of Ag-WO_3 core-shell nanostructures as efficient electrocatalysts for hydrogen evolution reaction, *Journal of Solid State Chemistry*, 271 (2019) 246-252.

[16] TAGHAVI POURIAN AZAR, G., REZAIE, H.R., GOHARI, B., RAZAVIZADEH, H. Synthesis and densification of W–Cu, W–Cu–Ag and W–Ag composite powders via a chemical precipitation method, *Journal of Alloys and Compounds*, 574 (2013) 432-436.

[17] STRAKOŠOVÁ, A., DVORSKÝ, D., PRŮŠA, F., MOLNÁROVÁ, O., HABR, S., SVOBODA, J., SEDLÁŘOVÁ, I., VOJTĚCH, D., LEJČEK, P. Microstructure and compression behavior of Ag–W metal matrix composite produced from core–shell powder by spark plasma sintering: case study, *The International Journal of Advanced Manufacturing Technology*, 139 (2025) 1571-1580.

[18] IMPELEN, D., GONZALES-GARCIA, L., KRAUS, T. Low-temperature sintering of Cu@Ag microparticles in air for recyclable printed electronics, *Journal of Materials Chemistry C*, 12 (2024) 12882.

[19] HAI, H.T., TAKAMURA, H., KOIKE, J. Oxidation behavior of Cu–Ag core–shell particles for solar cell applications, *Journal of Alloys and Compounds*, 564 (2013) 71-77.

[20] NAGY, D., HUMPRY-BAKER, S.A. An oxidation mechanism map for tungsten, *Scripta Materialia*, 209 (2022) 114373.

[21] PACCO, A., NAKANO, T., LOYO PRADO, J., LAI, J.-G., KAWARAZAKI, H., ALTAMINARO SANCHES, E. Etching of tungsten via a combination of thermal oxide formation and wet-chemical oxide dissolution, *Microelectronic Engineering*, 297 (2025) 112304.

[22] ROTTIER, B., REZEAU, H., CASANOVA, V., KOUZMANOV, K., MORITZ, R., SCHLÖGLOVA, K., WÄLLE, M., FONTBOTÉ, L. Trace element diffusion and incorporation in quartz during heating experiments, *Contributions to Mineralogy and Petrology*, 172 (2017) 23.

[23] LI, K., ZHU, R., LI, T., SHAN, X., LIU, J. First principles investigation on adsorption and diffusion of atomic oxygen on Ag surface, *Vacuum*, 238 (2025) 114268.

[24] MEHRER, H. Dependence of Diffusion on Temperature and Pressure, Diffusion in Solids: Fundamentals, Methods, Materials, Diffusion-Controlled Processes, Springer Berlin Heidelberg, Berlin, Heidelberg, (2007) 127-149.

[25] XIE, S., YU, M., CHEN, W., LU, G., LI, K., ZHAO, W. Research on the synthesis and sintering behavior of porous spherical silver particles, *Colloids and Surfaces A: Physicochemical and Engineering Aspects*, 708 (2025) 135950.

[26] VAN HERLE, J., MCEVOY, A.J. Oxygen diffusion through silver cathodes for solid oxide fuel cells, *Journal of Physics and Chemistry of Solids*, 55 (1994) 339-347.

[27] ALKHAMEES, A., LIU, Y.L., ZHOU, H.B., JIN, S., ZHANG, Y., LU, G.H. First-principles investigation on dissolution and diffusion of oxygen in tungsten, *Journal of Nuclear Materials*, 393 (2009) 508-512.

[28] GULBRANSEN, E.A., ANDREW, K.F. Kinetics of the Oxidation of Pure Tungsten from 500° to 1300°C, *Journal of The Electrochemical Society*, 107 (1960) 619.